Natural Halloysite@Si(CH$_2$)$_3$NH$_2$@Cu(acac)$_2$ as an efficient nanocatalyst for the one-pot and three-component synthesis of propargylamines under solvent-free conditions

Seyed Ali Mousavi-Mashhadi[1] · Kimia Hoseinzade[2] · Ali Shiri[1]

Abstract

A novel heterogeneous catalyst, natural halloysite@Si(CH$_2$)$_3$NH$_2$@Cu(acac)$_2$, was designed and synthesized through the functionalization of the halloysite nano clay surface by 3-aminopropyltriethoxysilane followed by copper acetylacetonate. The catalyst was characterized using various techniques such as FTIR, SEM, EDS, BET, ICP, XRD, TEM, and TGA. The catalytic activity of natural halloysite@ Si(CH$_2$)$_3$NH$_2$@Cu(acac)$_2$) was also evaluated for the synthesis of propargylamines using multicomponent A^3-coupling reaction of various aldehydes, amines, and phenylacetylene.

Keywords Functionalized halloysite · Propargylamines · Solvent-free reaction · A^3-coupling reaction

Introduction

Multicomponent reactions (MCRs) are becoming increasingly significant in organic chemistry for their ability to generate a wide range of structures from different components in a single step [1–3]. Among these MCRs, the A.^{3}-coupling of amines, alkynes, and aldehydes has received considerable interest in recent years as an effective method for producing propargylamine derivatives. These derivatives serve as versatile key intermediates for the synthesis of biologically active compounds and heterocyclic structures, including acrylamidines, oxazoles, and pyrroles [4–6].

✉ Ali Shiri
  alishiri@um.ac.ir; alimoosavi51@yahoo.com

  Kimia Hoseinzade
  kimia.hoseinzade@tu-clausthal.de

1 Department of Chemistry, Faculty of Science, Ferdowsi University of Mashhad, Mashhad, Iran

2 Institute of Organic Chemistry, Clausthal University of Technology, Leibnizstraße 6, 38678 Clausthal-Zellerfeld, Germany
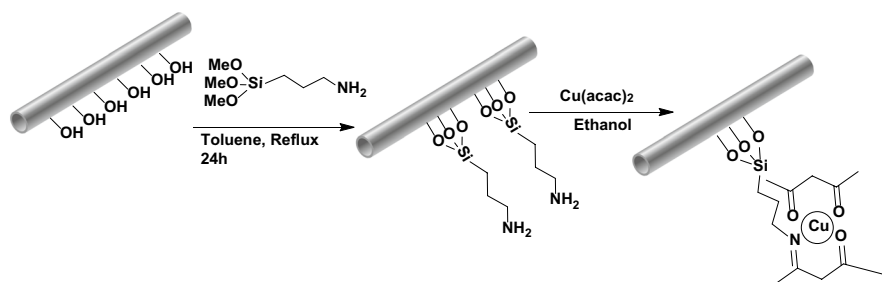
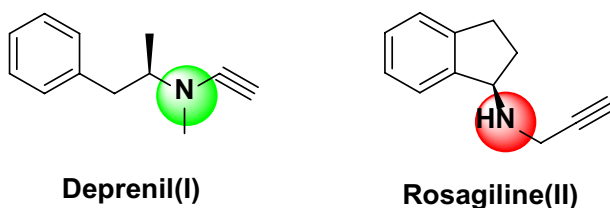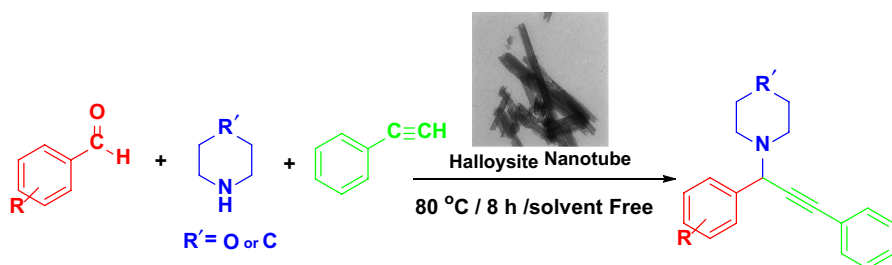**Scheme 1** Synthesis of H-AP-Cu catalyst

Fig. 1 Examples of propargylamines frame in drugs

Recent efforts have focused on developing one-pot MCRs with simple experimental procedures, utilizing inexpensive non-toxic materials, and reducing reaction times [7, 8]. Various transition metal-based catalytic systems involving iron, copper, silver, gold, and others [9–12] have played a crucial role in promoting these transformations [13]. Recently, heterogeneous catalysts, including silica gel anchored copper chloride [14, 15], copper ferrite nanoparticles [16], magnetic CuO nanoparticles supported on graphene oxide [17], and impregnated copper on magnetite [18–20], are also used for multicomponent reactions and A^3-coupling reactions. However, these methods are often associated with issues such as toxicity and the use of expensive or inaccessible materials (Scheme 1).

For effective A^3-coupling reactions, the development of new, efficient, environmentally friendly, and sustainable synthetic methods is highly anticipated [21–23] Notably, propargylamines have been utilized in the synthesis of Deprenil (I) and Rasagiline (II), which serve as monoamine oxidase inhibitors (MAOI) in the treatment of Alzheimer's [24, 25]. (Fig. 1).

Halloysite nanotubes (HNTs), with a general formula of $Al_2(OH)_4Si_2O_5.2H_2O$, are naturally occurring, nano-sized, and cost-effective materials found in mineral clay, sharing a similar structure with kaolinite [26–28]. These mesoporous tubular particulates demonstrate favorable adsorption and high loading capacities. The inner and outer surfaces of HNTs possess two types of hydroxyl groups, serving as active sites for drug loading and structural functionalization [29]. Recent attention has been drawn toward HNT-based nanocomposites, showing significant potential in various fields such as electronics, water treatment, gas separation, optics, and catalytic applications [8, 30–36] (Scheme 2).

Scheme 2 Synthesis of propargylamines using H-AP-Cu catalyst

Functionalized HNTs have been considered a reliable tool for broadening the applications of the HNTs and tuning their properties. Considering the presence of Cu(acac)$_2$ helps the catalyst to function through bonds instead of trapping between the pores [37]. Silane coupling linkers depend on the coordination of the surface and have found many properties and applications, especially with hydroxyl groups [38]. Moreover, functional groups including -OH and -NH$_2$ are performed to attach to other groups of catalyst [39].

Considering the aforementioned details and our recent research [2, 40–46], we propose an effective and distinctive catalyst for the synthesis of propargylamine derivatives via the A3-coupling reaction, resulting in satisfactory yields.

Results and discussion

In an effort to synthesize novel catalysts and establish practical and environmentally friendly methodologies for organic reactions, the structure of H-AP-Cu has been meticulously designed and characterized using various analytical techniques. These include Fourier transform infrared (FT-IR), X-ray diffraction (XRD), scanning electron microscopy (SEM), transmission electron microscopy (TEM), Brunauer–Emmett–Teller (BET), energy-dispersive X-ray (EDX), thermogravimetric (TGA), and inductively coupled plasma (ICP) analyses.

The preparation and characterization of the catalyst

FT-IR spectra of H-AP (halloysite/3-aminopropyltriethoxysilane), H-AP-Cu, and H-AP-Cu-R are recorded and compared with each other in Fig. 2. The obvious bands at 3697 and 3626 cm^{-1} can be assigned to internal and external OH groups of the catalyst. However, the bands at 536 and 1645 cm^{-1} are representatives of the Al–O–Si vibration and the interlayer water, respectively. Moreover, the conjugation of AMPTSi can be proved by the bands at 2927 and 1030 cm^{-1}, which are indicative of -CH$_2$ and Si–O stretching bands, respectively. As it is clear in the third spectra, there is no specific change for the recycled catalyst after six times of reaction (Fig. 2).
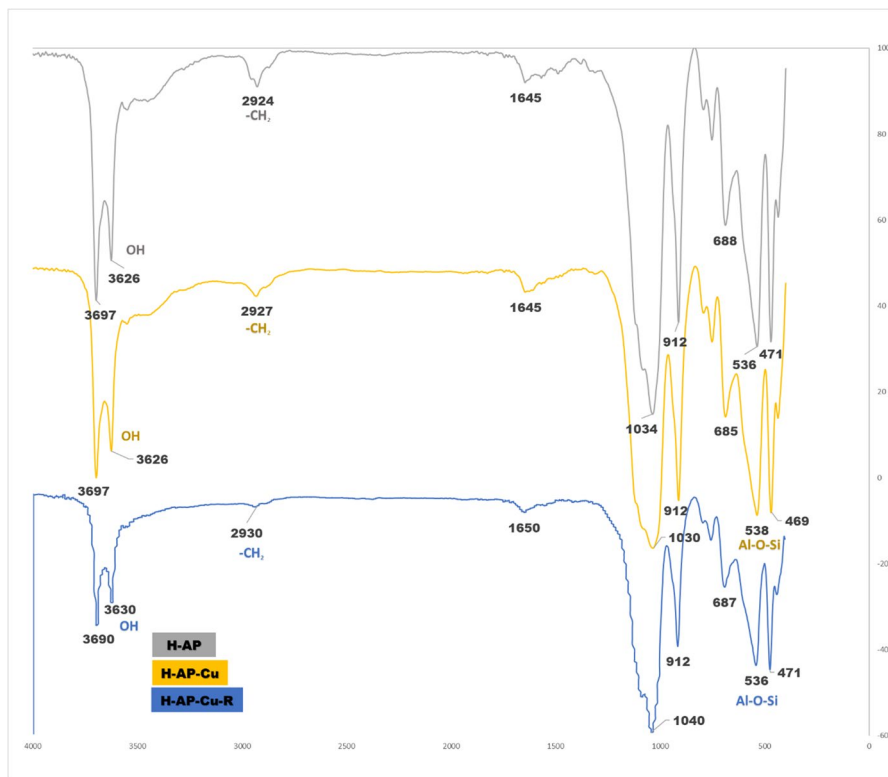
Fig. 2 The FTIR spectra of (**a**) H-AP, (**b**) H-AP-Cu, and (**c**) H-AP-Cu-R

The H-AP-Cu SEM images show the tubular morphology of the HNTs catalyst (Fig. 3). The characteristic of H-AP-Cu was also analyzed by TEM images (Fig. 4). The TEM image of H-AP-Cu represents a fine tubular structure that provides a high degree of active catalytic sites for efficient reactions and chemical transformation.

The EDX analyses for the catalyst confirmed the presence of Al, O, and Si that can be assigned to HNTs structure. The C and N atoms are representative of the AMPTSi complex. Also, the presence of Cu atoms proves the presence of copper acetylacetonate in the structure of the catalyst (Fig. 5).

The XRD pattern of H-AP-Cu is illustrated in Fig. 6. There are six diffraction peaks at 2θ about 20.07°, 35°, 35.88°, 37.94°, 52.53°, and 81.97° with indexes (1 1 0), (2 0 0), (1 1 3), (1 3 2), (1 1 5), and (4 0 5) lattice areas, respectively. The observed peaks confirm the tubular structure of the halloysite sample. Five peaks appear at 2θ about 11.89°, 20.96°, 37.94°, 52.53°, and 73.69° in the XRD pattern of H-AP-Cu that correspond to (1 0 1), (1 1 0), (1 1 4), (3 2 3), and (0 3 5) areas, respectively. No impurity was observed by XRD analysis of H-AP-Cu.

The TGA spectra of the H-AP-Cu catalyst are represented in Fig. 7, which is a necessary technique to find out the moisture and percentage of organic and
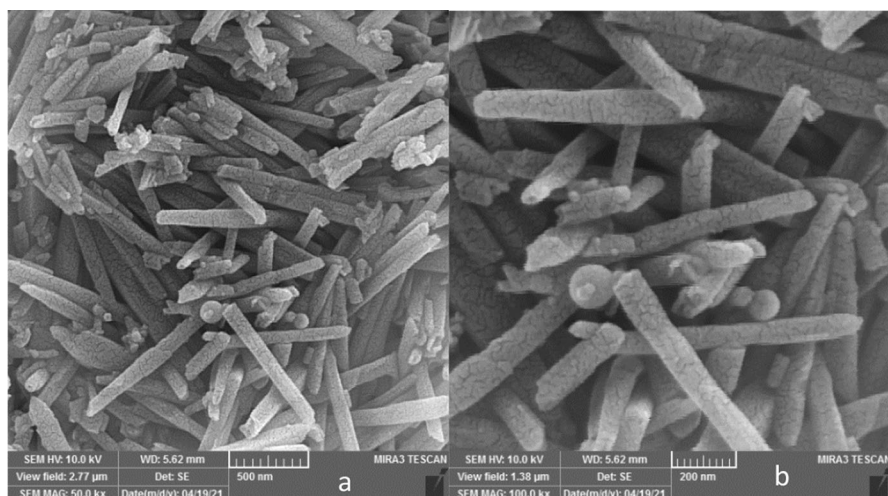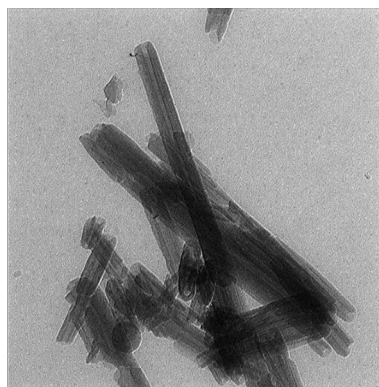
Fig. 3 The SEM analysis of H-AP-Cu catalyst (**a**) 500 nm (**b**) 200 nm

Fig. 4 The TEM image of
H-AP-Cu nanocatalyst

inorganic materials based on temperature. The first weight loss under 100 °C is attributed to the loss of H$_2$O and humidity. The second phase is related to the organic phase around 18.41%, which is allocated to decomposition starting at 300 °C and finishing at 550 °C.

The pore volume and specific surface area of H-Ap and H-AP-Cu catalysts were examined by BET analysis and indicated the surface areas of H-Ap and H-AP-Cu particles were 45.212 and 39.947 m^2 g^{-1}, respectively (Fig. 8).

The catalytic application of H-AP-Cu catalyst

The model reaction was optimized under various reaction conditions through a test reaction employing substrates such as benzaldehyde (1 mmol), morpholine (1 mmol), and phenylacetylene (1 mmol) (Table 1).
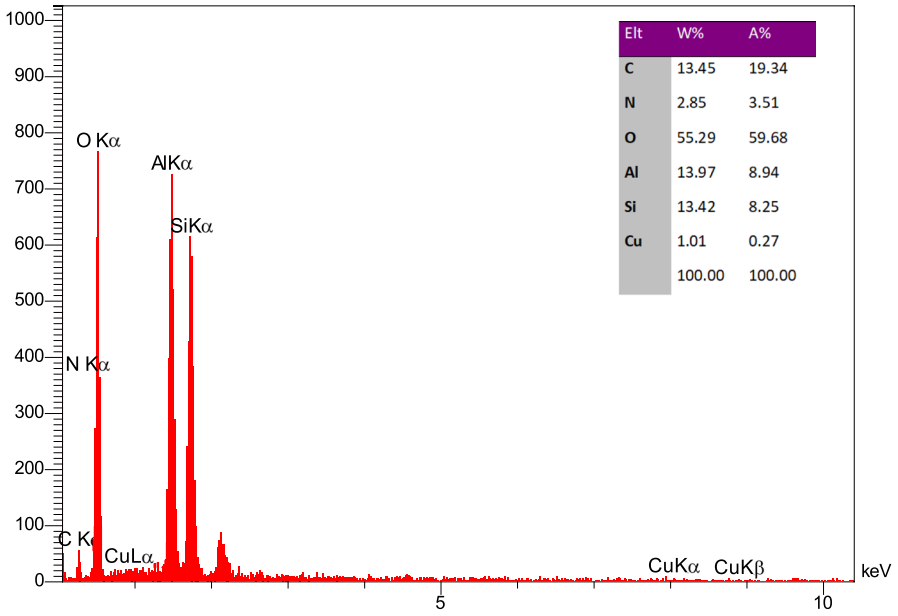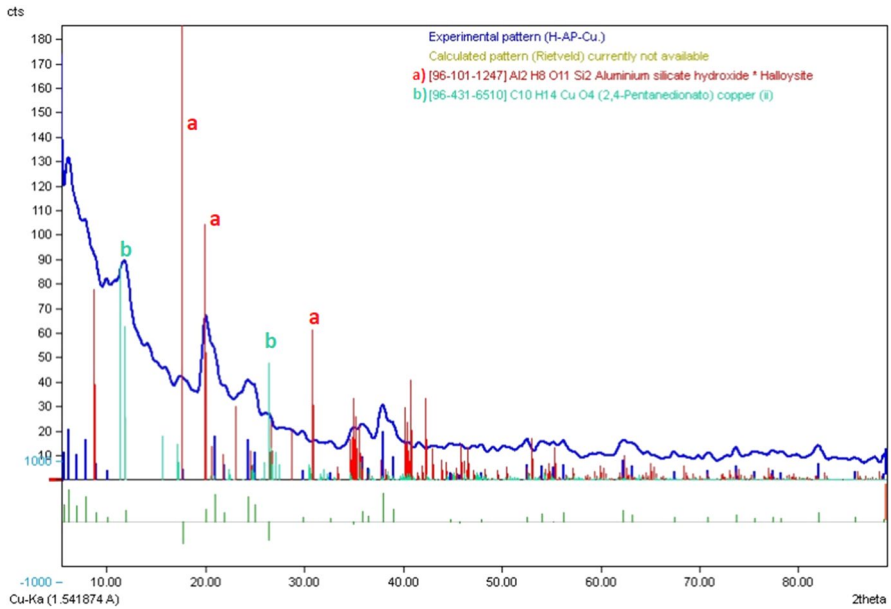
Fig. 5 The EDX analysis of H-AP-Cu

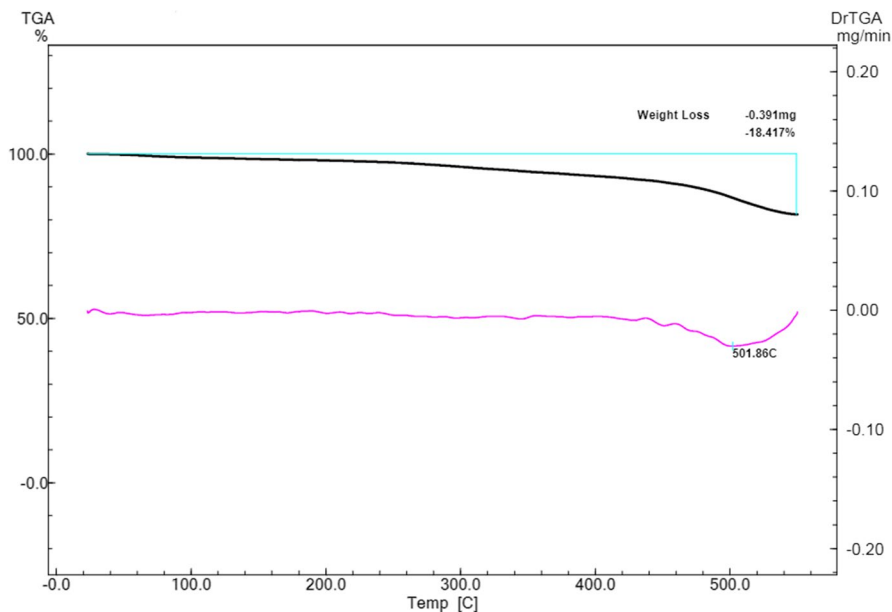**Fig. 6** The XRD pattern of the H-AP-Cu catalyst

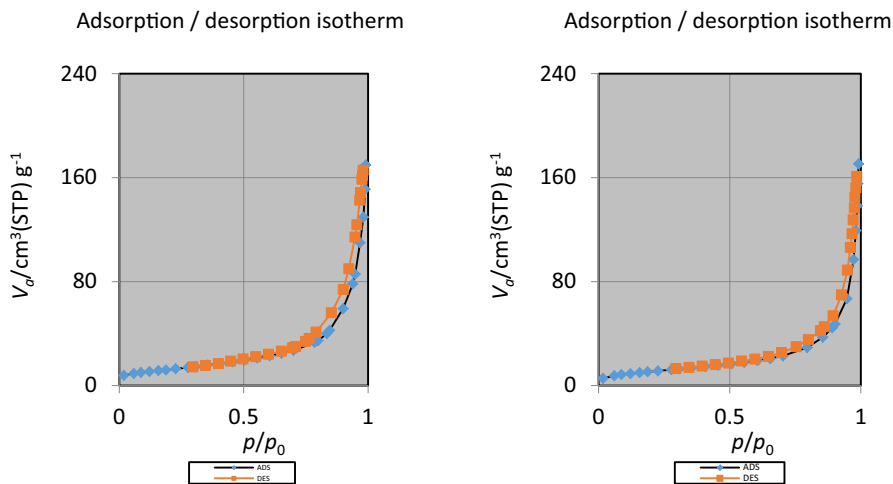**Fig. 7** The TGA analysis of the H-AP-Cu catalyst

Fig. 8 The BET analyses of H-Ap and H-AP-Cu catalysts

It is observed that the solvent-free conditions at 110 ℃ as well as in the absence of a catalyst resulted in no product formation even after 15 h. Next, carrying out the same reaction in the presence of a small amount of halloysite (5 mol%) resulted in 38% of product formation (Table 1, Entry 2). Several other similar conditions were then screened to obtain the best reaction yields. The effect of the catalyst has been examined, and it was found that the catalyst was

Table 1 The optimization of the reaction conditions for the model reaction
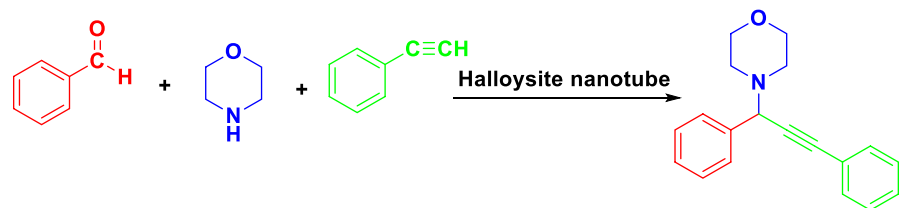
Entry	Catalyst (mg)	solvent	Temperature (ºC)	Time (h)	Yield (%)
1	0	Free	110	15	Trace
2	5	Free	110	15	38
3	5	DMF	Reflux	15	25
4	5	H$_2$O	Reflux	15	29
5	10	Free	100	15	77
6	10	Free	120	15	68
7	10	Free	Reflux	15	65
8*	**10**	**Free**	**80**	**8**	**96**
9	15	Free	80	8	96

* Optimized reaction conditions

able to moderately catalyze the reaction giving significant yields (Table 1). Further, the above reaction was also carried out in high boiling solvents such as DMF and water (Table 1, Entries 3 and 4). In water, it was noteworthy that no desirable yield was obtained even after prolonged reaction time. On carrying out the same reaction in solvent-free conditions at 100 °C for 15 h, it was also obtained 77% yield using 10 mol% of the halloysite. After choosing the solvent-free condition, various temperatures were focused on screening. Therefore, the use of halloysite (15 mol %) in solvent-free conditions for 8 h at 80 °C was selected to be the most suitable and perfect condition for this particular A^3-type coupling reaction. Moreover, employing a higher percentage of the catalyst has neither significantly increased the yield nor lowered the reaction time. After obtaining the optimized reaction conditions, namely aryl aldehyde (1 mmol), phenylacetylene (1 mmol), morpholine (1 mmol), and halloysite (10 mol%), in solvent-free condition at 80 ºC for 8 h, a wide range of available aryl aldehydes were tested. (Table 2) The mentioned reaction was also carried out using piperidine instead of morpholine, and it showed significant yields as represented in Table 2. Aryl aldehydes either withdrawing or donating groups resulted in the products with good to excellent yields.

The proposed mechanism for the synthesis of propargylamine is illustrated in Fig. 9, based on the reported catalyzed A3-coupling reaction. Initially, the activation of the alkyne by the catalyst is proposed. Subsequently, deprotonation occurs, leading to the formation of the alkyl-catalyst intermediate. This intermediate then coordinates with the in situ-generated iminium ion from the aldehyde and amine,
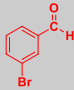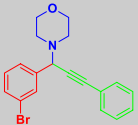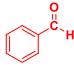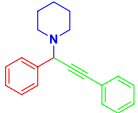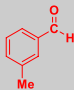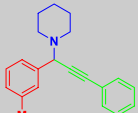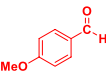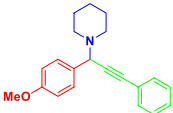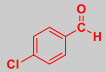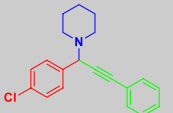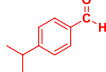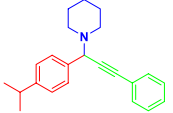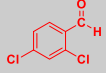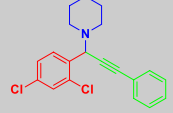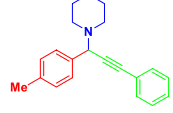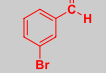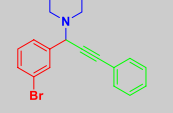
Table 2 The A³-coupling reaction of different aryl aldehydes, amines, and alkyne in the presence of H-AP-Cu catalyst

Entry	Aldehyde	Amine	Product	TON	TOF (h⁻¹)	Yield (%)
1		Morpholine		9.6	1.2	96
2		Morpholine		9.2	1.15	92
3		Morpholine		8.1	1.01	81
4		Morpholine		9.2	1.15	92
5		Morpholine		8.8	1.10	88
6		Morpholine		8.7	1.08	87
7		Morpholine		9.3	1.16	93

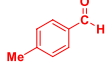forming the activated complex. The complex is further attacked by the alkyl-catalyst, resulting in the production of the corresponding product and the regeneration of the catalyst for the next cycle [47].

Table 2 (continued)

8		Morpholine		9.3	1.16	93
9		Piperidine		9.8	1.22	98
10		Piperidine		9	1.12	90
11		Piperidine		8	1	80
12		Piperidine		9.5	1.18	95
13		Piperidine		8.7	1.08	87
14		Piperidine		8.9	1.11	89
15		Piperidine		9.4	1.17	94
16		Piperidine		9.5	1.18	95

Reaction condition: Aldehyde (1 mmol), Amine (1 mmol), Alkyne (1 mmol), Catalyst (10 mg), Solvent-free, 80 ºC, 8 h
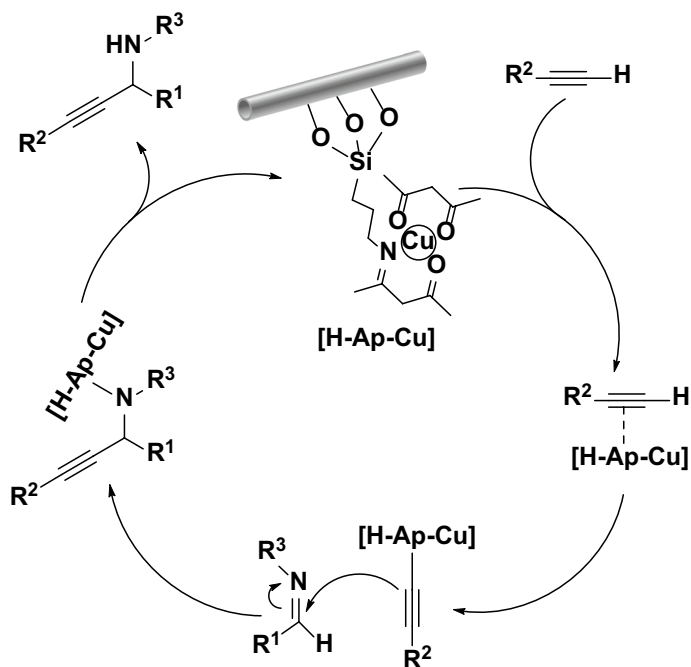
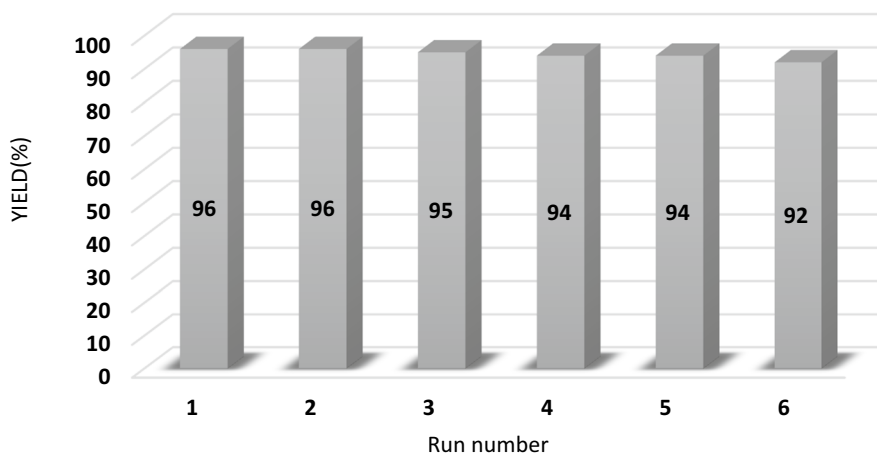**Fig. 9** The proposed mechanism for the A^3 coupling catalyzed by H-Ap-Cu

Fig. 10 The reusability of the H-AP-Cu catalyst

Table 3 The comparison of H-Ap-Cu for the synthesis of propargylamines derivatives with other reported ones in the literature

Entry	Conditions	Time	Yield (%)	[Lit.]
1	CuSO$_4$NPs@PEI/PTSAF/Solvent-free/120 °C	12 h	96	[48]
2	Cu-MPTA-nanocatalyst/CH$_2$Cl$_2$/rt	24 h	93	[49]
3	Cu nanoparticles/MeCN/ 100–110 °C/N$_2$	3.5–8 h	65–98	[50]
4	H-Ap-Cu/Solvent-free/80 °C	8 h	98	Current Work

The utilization of the catalyst H-AP-Cu has been examined in the optimized reaction condition; benzaldehyde (1.0 mmol), morpholine (1.0 mmol), phenylacetylene (1.0 mmol), and the catalyst. For this goal, after the completion of the reaction, the catalyst is separated from the reaction and reapplied in the subsequent reaction. The results obtained that the catalyst could be successively reused six times without any considerable loss in its activity (Fig. 10).

In addition, Table 3 compares the catalytic system efficiency for the reaction of aldehydes, amines, and alkynes with some of previously reported ones.

Conclusion

We have successfully synthesized a catalyst based on halloysite nanocomposites as a very stable and recoverable catalyst for the green production of propargylamine derivatives under the solvent-free conditions. The H-AP-Cu is an effective catalyst to be considered for the A^3-coupling reaction of aldehyde, amine, and phenylacetylene with nontoxic, perfect durability, reusability, shorter reaction time, and excellent product yields properties. The catalyst managed a wide variety of starting materials for the generation of propargylamine products in excellent yields.

Experimental

Synthesis of H-AP-Cu catalyst

A mixture of halloysite nanotubes (HNTs) (1.00 g) in dry toluene (50.0 mL) and (3-aminopropyl triethoxysilane (1 mL) was refluxed for 24 h. After the reaction was completed, the material was filtered off, washed with toluene (3 × 50 mL), and dried overnight in an oven at 70 °C. A solution of copper acetylacetonate (500 mg) in ethanol (100 mL, light blue solution) was refluxed with AMPTSi/HNTs for 24 h. At the end of the process, the color of the solution became slightly blue. The resulting solid was filtered off, washed with ethanol (3 × 20 mL) and dried in an oven at 60 °C.

General procedure for the synthesis of propargylamines using H-AP-Cu catalyst

A mixture of aldehyde (1.0 mmol), phenylacetylene (1.0 mmol), and amine (1.0 mmol) was prepared, to which the H-AP-Cu catalyst (10 mg) was added. The mixture was then heated at 80 °C under the solvent-free conditions for the appropriate reaction time. The progression of the reaction was monitored using TLC until the corresponding propargylamine derivatives were obtained. Subsequently, the catalyst was separated using a centrifuge and washed with ethanol (3×20 mL) and water (3×20 mL). The purified reaction products were obtained through silica gel column chromatography and confirmed using various spectroscopic analyses.

Declarations

Conflict of interest The authors declare no conflict of interest.

References

1. A. Bukowska, K. Bester, M. Pytel, W. Bukowski, Catal. Lett.. Lett. **151**, 422 (2021)
2. K. Hoseinzade, S.A. Mousavi-Mashhadi, A. Shiri, Mol. Divers. **5**, 2745 (2022)
3. A. Ying, S. Li, X. Liu, J. Wang, Y. Liu, Z. Liu, J. Catal. **391**, 312 (2020)
4. N. Nouruzi, M. Dinari, N. Mokhtari, B. Gholipour, S. Rostamnia, S. Khaksar, R. Boluki, Appl. Organomet. Chem. **34**, 5677 (2020)
5. A. Berrichi, Z. Bailiche, R. Bachir, Res. Chem. Intermed. **48**, 4119 (2022)
6. S. Peiman, R. Baharfar, R. Hosseinzadeh, Res. Chem. Intermed. **48**, 1365 (2022)
7. N. Esfandiary, F. Pazoki, A. Nakisa, K. Azizi, I. Radfar, A. Heydari, Appl. Organomet. Chem. **34**, 1 (2020)
8. M. Díaz-Sánchez, I. J. Gómez, S. Prashar, M. Horáček, M. Lamač, B. Urbán, J. Pinkas, and S. Gómez-Ruiz, Appl. Clay Sci. **214**, (2021).
9. J. Dulle, K. Thirunavukkarasu, M.C. Mittelmeijer-Hazeleger, D.V. Andreeva, N.R. Shiju, G. Rothenberg, Green Chem. **15**, 1238 (2013)
10. Y. He, M.F. Lv, C. Cai, Dalt. Trans. **41**, 12428 (2012)
11. X. Huo, J. Liu, B. Wang, H. Zhang, Z. Yang, X. She, P. Xi, J. Mater. Chem. A **1**, 651 (2013)
12. K. Namitharan and K. Pitchumani, Eur. J. Org. Chem. 411 (2010).
13. A. Bagherzade, F. Nemati, Res. Chem. Intermed. **47**, 2917 (2021)
14. B. Sreedhar, P. Surendra Reddy, C.S. Vamsi Krishna, P. VijayaBabu, Tetrahedron Lett. **48**, 7882 (2007)
15. A. Ying, M. Li, X. Lu, S. Li, L. Wang, Z. Liu, Y. Liu, Chem. Eng. J. **473**, 145361 (2023)
16. M. L. Kantam, J. Yadav, S. Laha, and S. Jha, Synlett. **11**, 1791 (2009)
17. M. Mirabedini, E. Motamedi, M.Z. Kassaee, Chinese Chem. Lett. **26**, 1085 (2015)

18. M.J. Aliaga, D.J. Ramón, M. Yus, Org. Biomol. Chem. **8**, 43 (2010)
19. S. Li, X. Lu, Q. Liu, L. Wang, Y. Liu, Z. Liu, A. Ying, J. Mater. Chem. A **10**, 3531 (2022)
20. X. Lu, S. Li, L. Wang, S. Huang, Z. Liu, Y. Liu, A. Ying, Fuel **310**, 122318 (2022)
21. A. Bukowska, W. Bukowski, K. Bester, K. Hus. Appl. Organomet. Chem. **31**, 3847 (2017)
22. S. Kujur, D. Deo, Res. Chem. Intermed. **46**, 369 (2019)
23. A. Rabiei, S. Abdolmohammadi, F. Shafaei, Zeitschrift Fur Naturforsch Sect. B J. Chem. Sci. **72**, 241 (2017)
24. F.T. Zindo, J. Joubert, S.F. Malan, Future Med. Chem. **7**, 609 (2015)
25. O. Weinreb, S. Mandel, O. Bar-Am, M. Yogev-Falach, Y. Avramovich-Tirosh, T. Amit, M.B.H. Youdim, Neurotherapeutics **6**, 163 (2009)
26. K. Fakhruddin, R. Hassan, M. Umar, A. Khan, S. Naula, S. Izwan, A. Razak, M. Hussni, H. Fitri, M. Latip, M. Najeb, A. Hassan, Arab. J. Chem. **14**, 103294 (2021)
27. S. Satish, M. Tharmavaram, D. Rawtani **6**, 1 (2019)
28. S. Sadjadi, S. Samadi, M. Samadi, Res. Chem. Intermed. **45**, 2441 (2019)
29. S. Sadjadi, M. M. Heravi, M. Malmir, F. Noritajer, Mater. Chem. Phys. **223**, 380 (2018)
30. N. Bahri-Laleh, S. Sadjadi, Res. Chem. Intermed. **44**, 6351 (2018)
31. M. Massaro, M. Casiello, L. D'Accolti, G. Lazzara, A. Nacci, G. Nicotra, R. Noto, A. Pettignano, C. Spinella, S. Riela, Appl. Clay Sci. **189**, 105527 (2020)
32. A.H. Zyoud, A. Zubi, S.H. Zyoud, M.H. Hilal, S. Zyoud, N. Qamhieh, A. Hajamohideen, H.S. Hilal, Appl. Clay Sci. **182**, 105294 (2019)
33. F. Jaberifard, M. Ghorbani, N. Arsalani, H. Mostafavi, Appl. Clay Sci. **230**, 106667 (2022)
34. H. Cheng, Z. Yang, F. Du, H. Liu, Q. Zhang, Y. Zhang, Appl. Clay Sci. **223**, 106510 (2022)
35. W. Zhang, X. Yan, Z. Liu, C. Du, Appl. Clay Sci. **224**, 106509 (2022)
36. M.V. Gorbachevskii, A.V. Stavitskaya, A.A. Novikov, R.F. Fakhrullin, E.V. Rozhina, E.A. Naumenko, V.A. Vinokurov, Appl. Clay Sci. **207**, 106106 (2021)
37. M. Ghavami, M. Koohi, M.Z. Kassaee, J. Chem. Sci. **125**, 1347 (2013)
38. D.G. Kurth, T. Bein, Langmuir **11**, 3061 (1995)
39. Y. Zhang, Z. Zhang, J. Li, G. Sui, Compos. Part B Eng. **169**, 148 (2019)
40. S.A. Mousavi-Mashhadi, A. Shiri, ChemistrySelect **6**, 3941 (2021)
41. K. Hoseinzade, S.A. Mousavi-Mashhadi, A. Shiri, J. Inorg. Organomet. Polym.Mater. **31**, 4648 (2021)
42. S.A. Mousavi-Mashhadi, M.Z. Kassaee, E. Eidi, Appl. Organomet. Chem. **33**, 1 (2019)
43. M. Keyhaniyan, A. Shiri, H. Eshghi, A. Khojastehnezhad, Appl. Organomet. Chem. **32**, 1 (2018)
44. M. Keyhaniyan, A. Shiri, H. Eshghi, A. Khojastehnezhad, New J. Chem. **42**, 19433 (2018)
45. S.A. Mousavi-Mashhadi, A. Shiri, Mol. Divers. **2**, 919 (2022)
46. S.A. Mousavi-Mashhadi, A. Shiri, J. Iran. Chem. Soc. **19**, 4523 (2022)
47. X. Liu, B. Lin, Z. Zhang, H. Lei, Y. Li, RSC Adv. **6**, 94399 (2016)
48. W. Jiang, J. Xu, W. Sun, Y. Li, Appl. Organomet. Chem. **35**, 1 (2021)
49. N. Salam, S.K. Kundu, A.S. Roy, P. Mondal, S. Roy, A. Bhaumik, S.M. Islam, Catal. Sci. Technol. **3**, 3303 (2013)
50. M. Kidwai, N.K. Mishra, V. Bansal, A. Kumar, S. Mozumdar, Tetrahedron Lett. **48**, 8883 (2007)